RESEARCH ARTICLE | FEBRUARY 19 2025

Transforming semitransparent organic photovoltaics into catalysts for positive emotional responses

Zonghao Wu; Jiangsheng Yu ; Wenxiao Wu; Zhenzhen Zhao; Siqi Ma ; Beibei Shi; Rui Shi; Xin Liu; Yuguo Chen; Ziwu Ji ; Feng Chen ; Xiaotao Hao ; Gang Li ; Hang Yin

Appl. Phys. Lett. 126, 073904 (2025)
https://doi.org/10.1063/5.0256211

Applied Physics Letters ARTICLE pubs.aip.org/aip/apl

Transforming semitransparent organic photovoltaics into catalysts for positive emotional responses

Cite as: Appl. Phys. Lett. **126**, 073904 (2025); doi: 10.1063/5.0256211
Submitted: 3 January 2025 · Accepted: 20 January 2025 ·
Published Online: 19 February 2025

View Online Export Citation CrossMark

Zonghao Wu,[1,2] Jiangsheng Yu,[3,4] Wenxiao Wu,[5] Zhenzhen Zhao,[1] Siqi Ma,[1] Beibei Shi,[1,2] Rui Shi,[1] Xin Liu,[4] Yuguo Chen,[5] Ziwu Ji,[2,a)] Feng Chen,[1] Xiaotao Hao,[1,a)] Gang Li,[3,a)] and Hang Yin[1,a)]

AFFILIATIONS

[1]School of Physics, State Key Laboratory of Crystal Materials, Shandong University, Jinan, Shandong 250100, China
[2]School of Integrated Circuits, Shandong University, Jinan, Shandong 250100, China
[3]Department of Electric and Electronic Engineering, Research Institute for Smart Energy (RISE), Photonic Research Institute (PRI), The Hong Kong Polytechnic University, Kowloon, Hong Kong 999077, China
[4]School of Electronic and Optical Engineering, Nanjing University of Science and Technology, Nanjing, Jiangsu 210094, China
[5]Department of Emergency Medicine, Qilu Hospital of Shandong University, Jinan, Shandong 250012, China

[a)]**Authors to whom correspondence should be addressed:** jiziwu@sdu.edu.cn; haoxt@sdu.edu.cn; gang.w.li@polyu.edu.hk; and hyin@sdu.edu.cn

ABSTRACT

Semitransparent organic photovoltaics (ST-OPVs), due to their transparency, can be integrated into building designs through building integrated photovoltaics (BIPVs) to address the energy challenges posed by urbanization. While current BIPVs such as photovoltaic windows meet the criteria for both the power supply and urban esthetics, a crucial aspect remains underexplored in the existing research: the human experience under such modulated sunlight. In this study, we conduct a systematic analysis of the interaction between spectrally tunable ST-OPV materials and human cognition and emotion, proposing a framework for selecting user-friendly ST-OPVs. Our results reveal that predominant high-performance donor polymer materials negatively influence user emotions. To address this issue, we employed spectrum shaping optical structures to optimize the device transmittance and color rendering properties, to achieve desirable human emotion feedback. This groundbreaking study delves into the user experience of ST-OPV devices, playing a crucial role in addressing the energy demands of urbanization and paving the way for the realization of smart, sustainable, and healthy cities.

The rapid urbanization projected to cover 70% people worldwide by 2050 poses significant challenges in the environmental and energy sectors, necessitating innovative solutions to address these complex issues.[1–5] Therefore, developing green urban energy systems that can replace traditional fossil fuels is crucial. These systems must not only be adaptable to the design of various types of urban buildings but also customizable to meet the diverse needs of different users. Semitransparent organic photovoltaic (ST-OPV) devices offer broad application potential, as they can be integrated into smart energy-generating windows, colorful skylights, greenhouses, and building facades.[6–10] These devices not only increase the solar energy collection area in cities but also enhance the esthetic appeal of buildings, making them a focal point of interest for researchers.

ST-OPV tunable spectral properties allow integrated windows to be customized for various urban infrastructures, such as office buildings, hospitals, and educational institutions, thereby facilitating power generation and regulating indoor lighting conditions.[11–16] Despite significant advancements in the power conversion efficiency (PCE) of semitransparent organic photovoltaic devices, the selection of photovoltaic systems for different urban scenarios remains unclear. While it is widely accepted that the use of white light in office environments can enhance concentration and work efficiency,[17,18] prevailing color analyses anchored in the CIE1931 standard overlooks the luminance of the transmitted light, a critical physical parameter for consumers. Consequently, the generalized spectrum of white light can elicit significantly different effects on individuals' emotional and physiological health. For example, Tzempelikos *et al.* found that neutral light rich in blue can enhance employee performance, while white light with higher saturation can increase employee error rates.[19] Kwallek *et al.* investigated the influences of interior colors on worker's

productivity and found the effects vary among different people and could have opposite impact on long-term and short-term productivity.[20] Therefore, understanding and optimizing the impact of ST-OPV devices on user visual interactions is a crucial step toward their commercialization, as for ST-OPV devices, user experience holds the same important position (or even more) compared to device performance.

In this work, we analyzed the impact of different ST-OPV devices from the perspective of urban building users and propose the requirements for ST-OPV devices in smart, green, and harmonious cities. Surprisingly, we observed that although donor polymers are one of the prerequisites for achieving high PCE in ST-OPV, their effects on user emotional feedback are negative. To examine the practical significance of ST-OPV modulation, we conducted biological experiments under various lighting conditions (open field tests with mice) and demonstrated that comfortable lighting conditions have diverse effects on mice behaviors. Subsequently, we analyzed the impact of a series of organic photovoltaic materials on smart windows and human emotions. Simply reducing donor materials proportion can quickly elicit positive emotional feedback from users, whereas the compensation is the reduced device performance. Therefore, we employed spectrum shaping optical structures to achieve a series of high-performance ST-OPV devices with desirable light utilization efficiency (LUE), color rendering index (CRI $>$ 97), and positive emotional feedback. This work explores the user experience of ST-OPV devices, offering a significant contribution to meeting the demands of urban environments and fostering the development of intelligent, sustainable, and healthy cities.

Figure 1(a) shows the color space diagram of CIE 1931, which is widely used in light source evaluation and currently used in the ST-OPV device field to characterize the color properties of devices. However, the CIE 1931 color space has limitations in representing certain colors (lacking a brightness dimension). For instance, as shown in Fig. S1, two shades of red with RGB values (255, 0, 0) and (125, 0, 0) share the same coordinates (0.64, 0.33) in the CIE 1931 space. Therefore, the CIE 1931 color space cannot distinguish between these two colors and does not provide accurate color properties, making it unsuitable for studying the emotional correlation of ST-OPV devices. Figure 1(b) shows the CIE Lab color space, which more accurately reflects perceptual color differences and is often used in color difference calculations (e.g., ΔE) and cross-device color matching. As can be seen from Fig. S1, it accurately distinguishes the different color characteristics of the two red colors. Hence, we propose a method to accurately obtain the color properties of semitransparent devices (detailed in the ESI). Based on the acquired color properties, we further provide a conversion method between color and PAD emotions[21] (with the corresponding color-emotion associations derived from statistical analysis). Based on the transmittance spectra of ST-OPV devices, the color characteristics of the devices can be determined. Then, by correlating the colors with the PAD emotional space, we can determine the PAD emotional coordinates of the ST-OPV devices. The corresponding calculation methods are detailed in the supplementary material. Figure 1(c) shows the PAD emotion space, which divides human emotions into eight quadrants based on PAD variations. The specific distribution of different emotions is shown in Table S1. Figure 1(d) demonstrates the impact of different color properties on PAD emotions. It can be observed that colors with high brightness and low saturation induce a sense of pleasure, leading designers to naturally incorporate these colors into their overall design. Subsequently, we analyzed different PAD emotion coordinates corresponding to a wide range of different colors (corresponding calculation methods are provided in ESI), as shown in Fig. 1(e).

To test the practical significance of photovoltaic window regulation, we designed an open field test for C57BL/6N mice under different light environments, with the experimental setup shown in Fig. 2(a). The illumination of different color light environments is controlled at 100 lux to avoid interference caused by illumination. Five mice were selected for each color light environment. If mice exhibit significant behavioral differences under different light environments, it indicates a correlation between light environments and biological emotions. Figures 2(b) and 2(c) show the heatmaps of time spent, movement paths of the mouse's central point, and instant movement speed for the entire duration of the test under red, green, and blue LED light environments. Typically, mice tend to move around the periphery due to thigmotaxis (preference for close contact with walls), but their curiosity about their surroundings leads them to explore the central area.[22–24] Therefore, mice with lower anxiety levels spend more time in the center. Conversely, mice with higher anxiety levels spend less time in the center. Analysis showed that under red light, mice spent more time in the central area, indicating lower anxiety levels in the red light environment. Figures 2(d)–2(j), respectively, depict the time spent in the center, total movement distance, average speed, and time spent in slow movement. Excited mice are more active, and, thus, their total movement distance and average speed increase. In contrast, depressed mice move less voluntarily, covering shorter distances with lower average speeds and spending more time in slow movement. Under red light, the total movement distance of mice increased, the average speed was higher, and the slow movement time was the shortest, indicating that the mice were more excited than other light conditions. Ultimately, the trajectory distribution map of mouse trajectories and voluntary movement monitoring show that mice exhibited higher excitement levels and lower depression levels under red light, confirming that different light environments, indeed, affect animal emotions. Therefore, the impact of different ST-OPV devices on human emotions is an issue that needs to be studied and addressed before their widespread application.

The analysis of the open field test for mice confirmed the impact of different color environments on animal emotions. Suitable color environments can help people work more efficiently and relax better, but it is still unclear which light environments are most suitable for humans. Therefore, we analyzed the PAD emotions of humans exposed to various light sources over a long period, such as sunlight, moonlight, and LEDs of different color temperatures, with their corresponding spectra shown in Fig. 3(a). These light sources correspond to PAD emotion coordinates of +P-A-D, representing calmness, compliance, and relaxation, as shown in Fig. S2. This is because sunlight, as the primary light source, has accompanied human evolution for millions of years.[25,26] During this time, the human body and its organs have adapted to sunlight, making it considered the healthiest and most comfortable light. Numerous studies have shown that sunlight can stimulate the brain to release neurotransmitters like serotonin, thereby enhancing mood and alleviating mental stress.[27–32] Consequently, we set the +P-A-D emotional coordinates associated with sunlight as the optimization direction for semitransparent devices. Moonlight, essentially reflected sunlight, and LEDs of different color temperatures

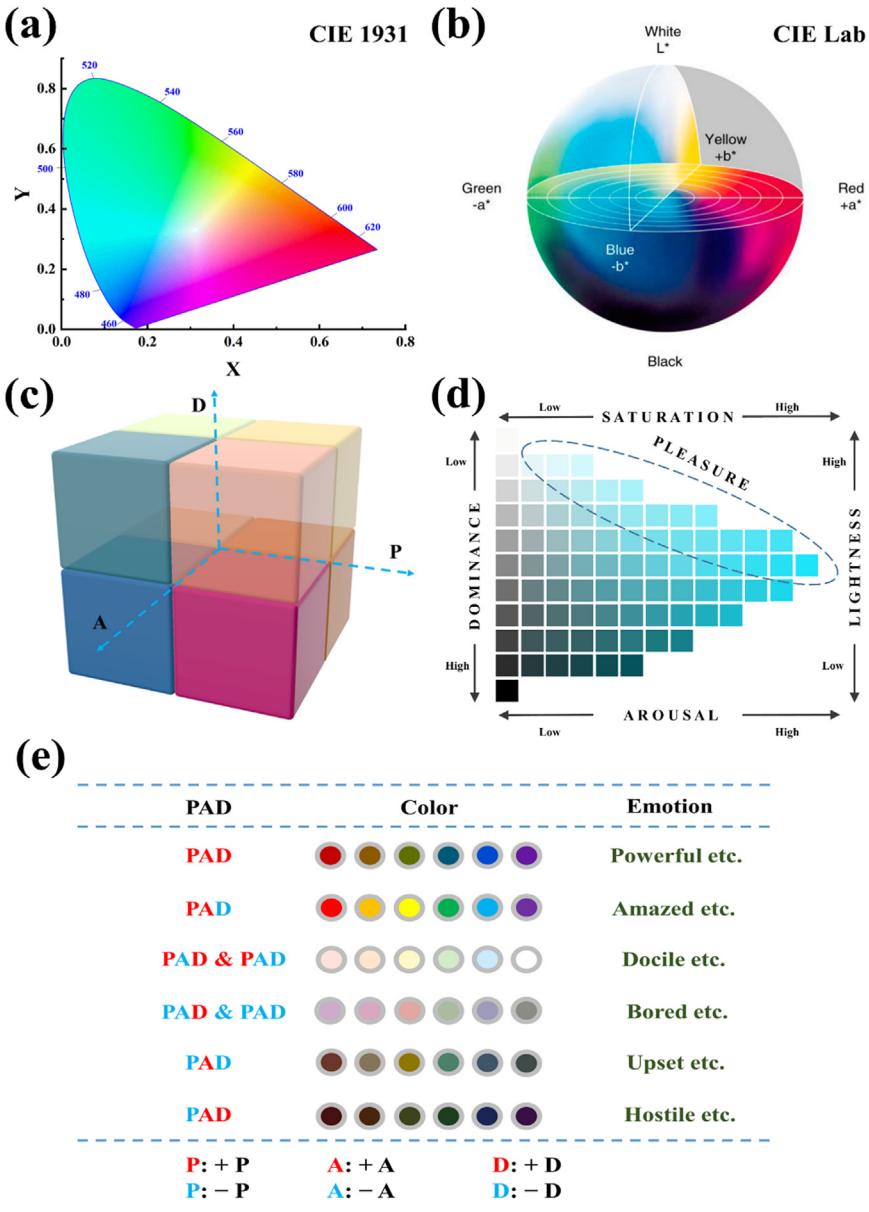

FIG. 1. (a) CIE 1931 Color Space. (b) CIE Lab color space. (c) PAD emotional space. (d) Diagram of the relationship between PAD emotion and color brightness and saturation. (e) Example diagram of the correlation between different PAD coordinates and colors.

correspond to the perception of sunlight at different times of the day. They all achieve visual comfort similar to sunlight, thus obtaining the +P-A-D emotional coordinates. Therefore, appropriate ST-OPV devices should have visual comfort comparable to sunlight to achieve user emotions like relaxation and compliance (+P-A-D emotion coordinates).

Next, we analyzed the color characteristics and PAD emotion coordinates of different ST-OPV materials. Figure 3(b) shows the color brightness and saturation of these materials and different light sources. It can be seen that small molecule acceptor materials and light sources have high brightness and low saturation. In contrast, donor polymer materials exhibit low brightness and high saturation. Figure 3(c) is a CIE Lab diagram, where the value of a^* corresponds to the change from green to red, and the value of b^* corresponds to the change from blue to yellow. The values of a^* and b^* range from −100 to 100, and when both are zero, it corresponds to white. From the figure, it is clear that acceptor materials and light sources are concentrated in the central region (0,0), whereas donor materials are more distributed toward the periphery. This is because the light absorption of acceptor materials is concentrated in the non-visible region (as shown in Fig. S3), making the transmission spectrum of visible light more uniform. On the other hand, the light absorption of donor materials is mainly in the visible light region (as shown in Fig. S4), resulting in uneven transmission of visible light and more diverse color properties. In general, the intensity of the transmission spectrum of devices affects the brightness, and the uniformity of the transmission spectrum affects the saturation. Although BTA3 and ITIC are acceptor materials, their absorption

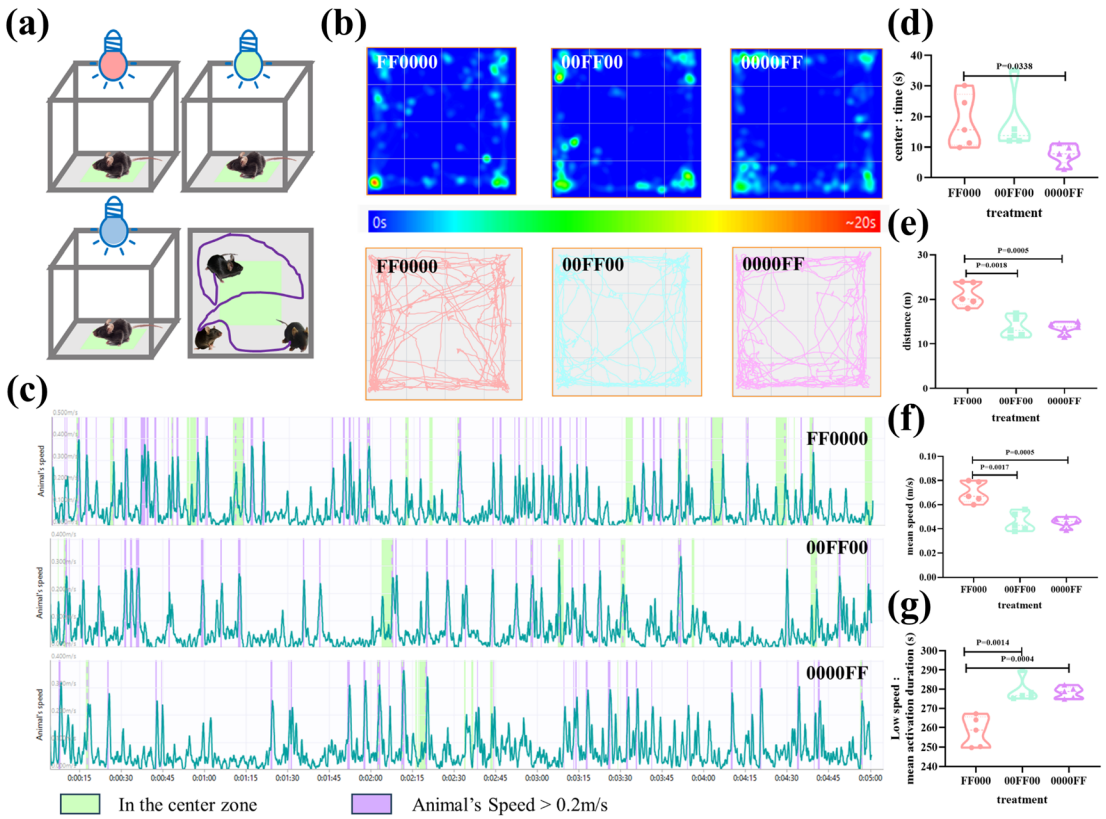

FIG. 2. (a) Schematic diagram of open field test (40 × 40 cm^2 floor). (b) Representative heatmaps of time spent and representative movement paths of the mouse's central point for the entire duration of the test under red (FF0000), green (00FF00), and blue (0000FF) light fields. (c) Representative instant movement speed of the mouse. Moving in the central zone marked with green and instant movement speed higher than 0.2 m/s marked with purple. (d) Central residence time, (e) total travel distance, (f) mean speed, and (g) low speed (<0.2 m/s) duration time in the test under different light fields.

peaks are similar to those of donor materials, focusing on the visible light region of 500–700 nm. Therefore, the saturation and brightness of the transmittance spectrum are closer to that of the donor material, and the corresponding emotional results are different from those of other acceptor materials. Figures 3(d) and 3(e) show the PAD emotion coordinates corresponding to different light sources and ST-OPV materials. Light sources and most acceptor materials exhibit +P-A-D emotion coordinates (associated with relaxation and docility), whereas donor materials exhibit +P+A-D emotion coordinates, differing from sunlight.

The analysis of Fig. 3 indicates that donor and acceptor materials generate +P+A-D and +P-A-D emotion coordinates, respectively. Therefore, we studied the emotional changes in humans corresponding to ST-OPV devices by adjusting the D:A ratio. To prepare high-performance ST-OPV devices, we selected PM6:BTP-eC9 as the active layer and fabricated devices with weight ratios of 1:1.2, 0.8:1.2, 0.5:1.2, 0.2:1.2, and 0:1.2. Figures S4(a)–S4(d) show the *J-V* curves, transmittance spectra, CIE Lab coordinates, and PAD emotion coordinates of ST-OPV devices under different D:A ratios. More detailed *J-V* parameters are shown in Table S2. From Figs. S4(a) and S4(b), it can be seen that reducing the donor ratio increases the transmittance of the ST-OPV device in the visible region, but the PCE gradually decreases. As the donor ratio decreases from 1 to 0, the CIE Lab coordinates move toward the central region (0,0), and the PAD emotion coordinates of the ST-OPV device shift from +P+A-D to +P-A-D, matching the PAD emotion coordinates of sunlight. This change occurs because the brightness of the device transmission spectrum correlates positively with its integrated intensity in the visible region, while color saturation correlates negatively with the uniformity of the transmission spectrum (with sunlight having a brightness of 100 and saturation of 0). Ultimately, a low donor ratio enhances the device visible light transmission spectrum, increasing the transmission spectrum brightness and reducing saturation, thus achieving the +P-A-D emotion coordinates. Finally, under experimental conditions of 5000 rpm, the device with a D/A ratio of 0.2:1.2 achieved the +P-A-D emotion coordinates, whereas the corresponding PCE was only 0.73%, as shown in Fig. S5 and Table S3. Thus, while adjusting the D:A ratio of ST-OPV devices can generate emotion coordinates similar to sunlight, i.e., +P-A-D emotion coordinates, the PCE of the device is very low, and therefore, the D:A tuning is not an effective strategy to address this issue.

The aperiodic bandpass filters (ABPFs) can increase the AVT while maintaining PCE, resulting in higher LUE values.[13] To optimize the PAD emotion coordinates while maintaining device performance, we adopted the ABPF structure. Figures 4(a) and S7 show the *J-V* curves, transmittance spectra, and EQE of ST-OPV devices with different active layer thicknesses. The device structure is shown in Fig. S8,

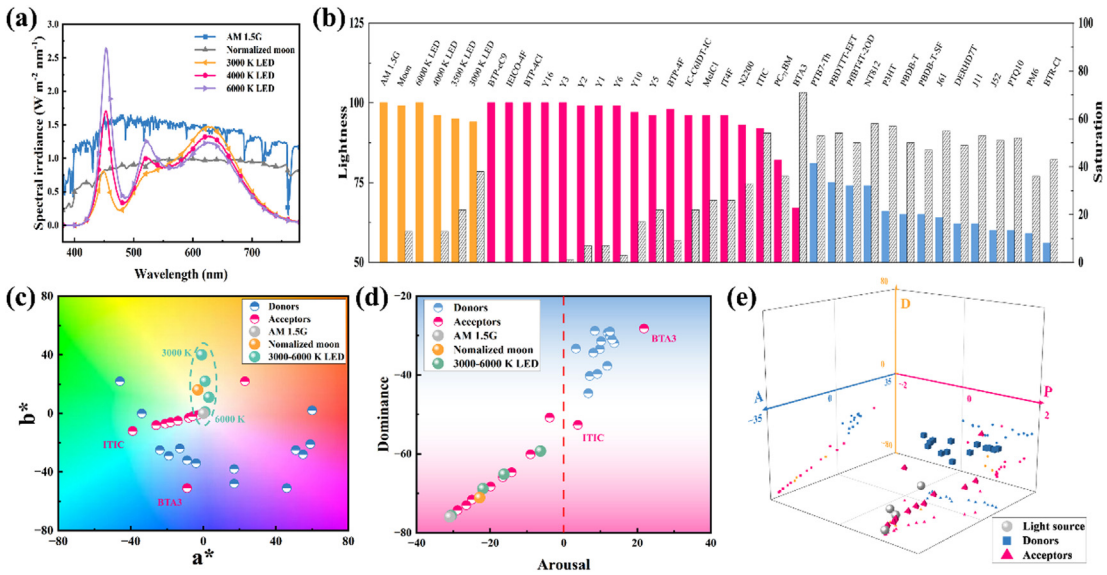

FIG. 3. (a) Power distribution of different light sources. (b) Brightness and saturation, (c) CIE Lab coordinates, (d) arousal and dominance, and (e) PAD emotional coordinates of different ST-OPV materials and light sources.

with detailed parameters provided in Tables S4–S6. As the active layer thickness decreases, the increase in AVT outweighs the reduction in PCE, allowing the LUE value to improve. All thicknesses achieved over 12% PCE, 25% AVT, and 3.80% LUE. Figures 4(b)–4(d) show the CIE color coordinate diagram and digital photographs of different devices. In addition to the high LUE devices, two sets of high CRI devices (CRI > 97) using the Fabry–Pérot resonant optical coating (FPOC) structure are included. Detailed parameters and performance of these devices are shown in Fig. S9 and Tables S7 and S8. The best color rendering device achieved a CRI of 99.23 and an LUE of 3.55%. From the CIE 1931 diagram [Fig. 4(b)], it can be seen that as the active layer thickness decreases, the coordinates of high LUE devices gradually

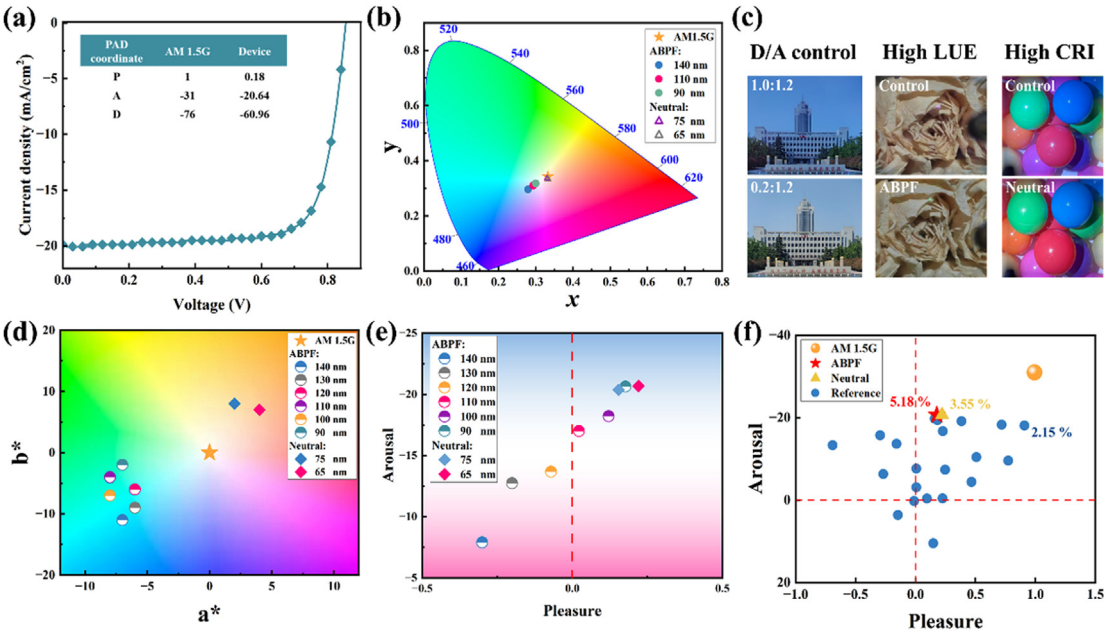

FIG. 4. (a) *J-V* curve of 90 nm active layer ST-OPV devices. (b) CIE 1931 coordinates, (c) digital photographs, (d) CIE Lab coordinates, and (e) PAD emotional coordinates of different ST-OPV devices. (f) PAD emotional coordinates of ST-OPV devices from literatures and this work.

approach those of sunlight. The coordinates of high CRI devices are almost identical to those of sunlight. As shown in Fig. 4(d), with decreasing active layer thickness, the a∗ value of high LUE devices remains relatively constant, while the b∗ value increases from −11 to −2, gradually approaching the coordinates of sunlight (0, 0). Figure 4(e) shows the PAD emotion coordinates of devices with different thicknesses. Although devices with thicknesses of 120–150 nm achieve more than 14.50% PCE, their PAD emotion coordinates are -P-A-D, corresponding to negative emotions like boredom, depression, and lack of interest. As the active layer thickness further decreases to 110 nm, the PCE drops to 14.16%, AVT increases from 31.12% to 34.45%, and LUE rises from 4.54% to 4.88%. The increase in AVT leads to higher brightness in the transmittance spectrum (positively correlated with the integral of the transmittance spectrum), causing the PAD emotion coordinates to shift from -P-A-D to +P-A-D. This change indicates a transition from negative to positive emotions, aligning with the emotional coordinates of sunlight. As the thickness of the active layer decreases, the PAD coordinates of the device will move closer to the sunlight coordinates. Additionally, the LUE values of these devices all exceed 4.80%. The PAD coordinates of high CRI devices also lie in the +P-A-D region. Figure 4(f) shows the PAD emotion coordinates from different literatures. In the figure, the LUE of the device closest to sunlight PAD emotional coordinate is 2.15%. Compared to other works, this work achieved high-performance devices with PAD emotional coordinates closer to sunlight while maintaining a 5.18% LUE. This enables ST-OPV devices to simultaneously meet urban energy needs and provide user visual comfort.

In this work, we established a correlation between ST-OPV devices and the perception of urban building users. Our analysis indicates that the visual effects of sunlight, moonlight, and LEDs with a color temperature range of 3000–6000 K contribute to emotions such as relaxation and calmness. Subsequent device analysis indicated that the high-performance donor polymers currently used in ST-OPV devices play a significant role in determining the emotional impact on users exposed to different lighting environments. However, their influence on user emotions is negative. Simply reducing donor proportion can quickly yield positive emotional feedback from users, whereas the compensation is the reduced device performance. Therefore, we adopted spectrum shaping optical structures to fabricate a series of ST-OPV devices with desirable LUE (>4.80%), CRI (>99 with 3.55% LUE), and positive emotional feedback. This work explores the user experience of ST-OPV devices, providing a significant contribution to the realization of smart, sustainable, and healthy cities.

See the supplementary material for PAD emotion coordinate calculation, open field test, and experimental details, including performance optimization and other characterizations for ST-OPV devices.

This work was financially supported by the National Natural Science Foundation of China (Grant No. 12204272). H.Y. acknowledges the Shandong Provincial Natural Science Foundation (No. ZR2022YQ04) and the Qilu Young Scholar Program of Shandong University.

AUTHOR DECLARATIONS

Conflict of Interest

The authors have no conflicts to disclose.

Author Contributions

Zonghao Wu, Jiangsheng Yu, Wenxiao Wu, and Zhenzhen Zhao contributed equally to this work.

Zonghao Wu: Conceptualization (equal); Data curation (equal); Formal analysis (lead); Writing – original draft (lead). **Jiangsheng Yu:** Data curation (equal). **Wenxiao Wu:** Data curation (equal). **Zhenzhen Zhao:** Data curation (equal). **Siqi Ma:** Data curation (supporting). **Beibei Shi:** Data curation (supporting). **Rui Shi:** Data curation (supporting). **Xin Liu:** Data curation (supporting). **Yuguo Chen:** Writing – review & editing (supporting).**Ziwu Ji:** Writing – review & editing (equal). **Feng Chen:** Writing – review & editing (supporting). **Xiaotao Hao:** Writing – review & editing (equal). **Gang Li:** Writing – review & editing (equal). **Hang Yin:** Conceptualization (equal); Funding acquisition (lead); Writing – review & editing (equal).

DATA AVAILABILITY

The data that support the findings of this study are available within the article and its supplementary material.

REFERENCES

[1]S. Wang, X. Bai, X. Zhang, S. Reis, D. Chen, J. Xu, and B. Gu, Nat. Food **2**, 183–191 (2021).
[2]L. Jiang and B. C. O'Neill, Glob. Environ. Change-Hum. Policy Dimens. **42**, 193–199 (2017).
[3]H. Liu, C. Fang, Y. Miao, H. Ma, Q. Zhang, and Q. Zhou, J. Geogr. Sci. **28**, 919–936 (2018).
[4]L. Chen, L. Huang, J. Hua, Z. Chen, L. Wei, A. I. Osman, S. Fawzy, D. W. Rooney, L. Dong, and P.-S. Yap, Environ. Chem. Lett. **21**, 1627–1657 (2023).
[5]J. Peng, J. Yan, Z. Zhai, C. N. Markides, E. S. Lee, U. Eicker, X. Zhao, T. E. Kuhn, M. Sengupta, and R. A. Taylor, Appl. Energy **264**, 114740 (2020).
[6]Y. Li, X. Huang, H. K. M. Sheriff, Jr., and S. R. Forrest, Nat. Rev. Mater. **8**, 186–201 (2022).
[7]Y. Li, J. Wang, C. Yan, S. Zhang, N. Cui, Y. Liu, G. Li, and P. Cheng, Joule **8**, 527–541 (2024).
[8]Z. Wu, B. Shi, J. Yu, M. Sha, J. Sun, D. Jiang, X. Liu, W. Wu, Y. Tan, H. Li, S. Huang, J. Wang, J. Liu, C. Zhang, X. Ma, L. Cui, L. Ye, F. Zhang, B. Cao, Y. Chen, Z. Ji, F. Chen, X. Hao, G. Li, and H. Yin, Energy Environ. Sci. **17**, 6013–6023 (2024).
[9]H. Yu, J. Wang, Q. Zhou, J. Qin, Y. Wang, X. Lu, and P. Cheng, Chem. Soc. Rev. **52**, 4132–4148 (2023).
[10]W. Kong, J. Wang, Y. Hu, N. Cui, C. Yan, X. Cai, and P. Cheng, Angew. Chem., Int. Ed. **135**, e202307622 (2023).
[11]S. Liu, H. Li, X. Wu, D. Chen, L. Zhang, X. Meng, L. Tan, X. Hu, and Y. Chen, Adv. Mater. **34**, 2201604 (2022).
[12]Q. Zhou, C. Yan, H. Li, Z. Zhu, Y. Gao, J. Xiong, H. Tang, C. Zhu, H. Yu, S. P. G. Lopez, J. Wang, M. Qin, J. Li, L. Luo, X. Liu, J. Qin, S. Lu, L. Meng, F. Laquai, Y. Li, and P. Cheng, Nano-Micro Lett. **16**, 224 (2024).
[13]X. Liu, Z. Zhong, R. Zhu, J. Yu, and G. Li, Joule **6**, 1918–1930 (2022).
[14]W. He, H. Li, R. Ma, X. Yan, H. Yu, Y. Hu, D. Hu, J. Qin, N. Cui, J. Wang, S. Lu, C. Yan, G. Li, and P. Cheng, Adv. Funct. Mater. **34**, 2313594 (2024).
[15]S. S. Dipta, J. Schoenlaub, M. H. Rahaman, and A. Uddin, Appl. Energy **328**, 120208 (2022).
[16]W. Song, J. Ge, L. Xie, Z. Chen, Q. Ye, D. Sun, J. Shi, X. Tong, X. Zhang, and Z. Ge, Nano Energy **116**, 108805 (2023).
[17]Y. Al Horr, M. Arif, A. Kaushik, A. Mazroei, M. Katafygiotou, and E. Elsarrag, Build. Environ. **105**, 369–389 (2016).
[18]M. Motamedzadeh, R. Golmohammadi, R. Kazemi, and R. Heidarimoghadam, Physiol. Behav. **177**, 208–214 (2017).
[19]I. Konstantzos, S. A. Sadeghi, M. Kim, J. Xiong, and A. Tzempelikos, Energy Build. **226**, 110394 (2020).
[20]N. Kwallek, K. Soon, and C. M. Lewis, Color Res. Appl. **32**, 130–143 (2007).

[21]P. Valdez and A. Mehrabian, "Effects of color on emotions," J. Exp. Psychol.-Gen. **123**, 394–409 (1994).
[22]T. D. Gould, D. T. Dao, and C. E. Kovacsics, "The open field test," in *Mood and Anxiety Related Phenotypes in Mice: Characterization using Behavioral Tests* (Springer, 2009), Vol. 42, pp. 1–20.
[23]K. M. McAteer, F. Corrigan, E. Thornton, R. J. Turner, and R. Vink, PLoS One **11**, e0160220 (2016).
[24]L. B. Tucker and J. T. McCabe, Front. Behav. Neurosci. **15**, 682935 (2021).
[25]M. Feelisch, V. Kolb-Bachofen, D. Liu, J. O. Lundberg, L. P. Revelo, C. V. Suschek, and R. B. Weller, Eur. Heart J. **31**, 1041–1045 (2010).
[26]G. W. Lambert, C. Reid, D. M. Kaye, G. L. Jennings, and M. D. Esler, Lancet **360**, 1840–1842 (2002).
[27]S. L. McColl and J. A. Veitch, Psychol. Med. **31**, 949–964 (2001).
[28]T. Partonen and J. Lönnqvist, J. Affect. Disord. **57**, 55–61 (2000).
[29]N. Praschak-Rieder, M. Willeit, A. A. Wilson, S. Houle, and J. H. Meyer, Arch. Gen. Psychiatry **65**, 1072–1078 (2008).
[30]L. Welberg, Nat. Rev. Neurosci. **8**, 812–812 (2007).
[31]N. Yamada, M. T. Martiniverson, K. Daimon, T. Tsujimoto, and S. Takahashi, Biol. Psychiatry **37**, 866–873 (1995).
[32]S. N. Young, J. Psychiatry Neurosci. **32**, 394–399 (2007).